

Table 5
Correlation of material properties with age, body weight, bone length, cortical bone mineral density, and histomorphometric parameters in the tibial diaphyses

	Breaking stress (n = 16)	Elastic modulus (n = 16)	Toughness (n = 16)
<i>Age, body weight, and bone length</i>			
Age	-0.503 (0.253)*	-0.049 (0.002)	-0.442 (0.196)
Body weight	0.129 (0.017)	0.138 (0.019)	-0.165 (0.027)
Bone length	0.452 (0.205)	-0.208 (0.043)	0.111 (0.012)
<i>Bone densitometry in the right tibiae</i>			
Total-Ct.BMD	0.630 (0.397)*	0.479 (0.229)	-0.500 (0.250)*
Anterior-Ct.BMD	0.504 (0.254)	0.659 (0.435)*	-0.306 (0.094)
Posterior-Ct.BMD	0.579 (0.335)*	0.489 (0.239)	-0.626 (0.392)*
<i>Bone histomorphometry in the left tibiae</i>			
Anterior region			
On.Dn	-0.135 (0.018)	-0.345 (0.119)	0.228 (0.052)
%On.Ar	-0.228 (0.052)	-0.453 (0.205)	-0.048 (0.002)
%On.B.Ar	-0.220 (0.049)	-0.468 (0.219)	-0.042 (0.002)
%Il.On.Ar	-0.175 (0.031)	-0.437 (0.191)	-0.065 (0.004)
%Sd.On.Ar	-0.233 (0.055)	-0.322 (0.104)	-0.004 (<0.001)
Po	-0.248 (0.061)	-0.404 (0.163)	-0.058 (0.003)
%O.Ar	0.327 (0.107)	0.090 (0.008)	-0.051 (0.003)
Posterior region			
On.Dn	-0.358 (0.128)	-0.424 (0.180)	0.494 (0.244)
%On.Ar	-0.298 (0.089)	-0.581 (0.338)*	0.511 (0.261)*
%On.B.Ar	-0.271 (0.073)	-0.566 (0.321)*	0.504 (0.254)*
%Il.On.Ar	-0.321 (0.103)	-0.528 (0.278)*	0.450 (0.202)
%Sd.On.Ar	-0.019 (<0.001)	-0.495 (0.245)	0.501 (0.251)*
Po	-0.407 (0.165)	-0.415 (0.172)	-0.179 (0.032)
%O.Ar	0.297 (0.088)	0.387 (0.150)	-0.115 (0.013)

Breaking stress, elastic modulus, and toughness were measured in the right tibiae. Ct.BMD, cortical bone mineral density; On.Dn, osteon population density; %On.Ar, percent osteonal area; %On.B.Ar, percent osteonal bone area; %Il.On.Ar, percent osteonal area of initial remodeling; %Sd.On.Ar, percent osteonal area of secondary remodeling; Po, porosity; %O.Ar, percent osteoid area. Asterisk shows significant correlation (level of significance: $P < 0.05$). Parentheses: coefficient of determination (r^2). The significant relationships between Ct.BMD and each property are also graphed in Fig. 2.

positively correlated with toughness. On the other hand, in the anterior region, there were no significant correlations between the values of bone histomorphometry and the mechanical properties of bone material. Backward stepwise multiple regression analyses indicated that posterior-Ct.BMD and total-Ct.BMD were the best variables to predict breaking stress and toughness, respectively, after entering the effect of

age. The final model for elastic modulus was the same as that produced using simple regression analysis (Table 6).

Relationship between pQCT and bone histomorphometry

The correlation coefficients between the values of pQCT and histomorphometric parameters are shown in Table 7. In the posterior region, among the histomorphometric parameters, %On.Ar, %On.B.Ar, and %Il.On.Ar were negatively correlated

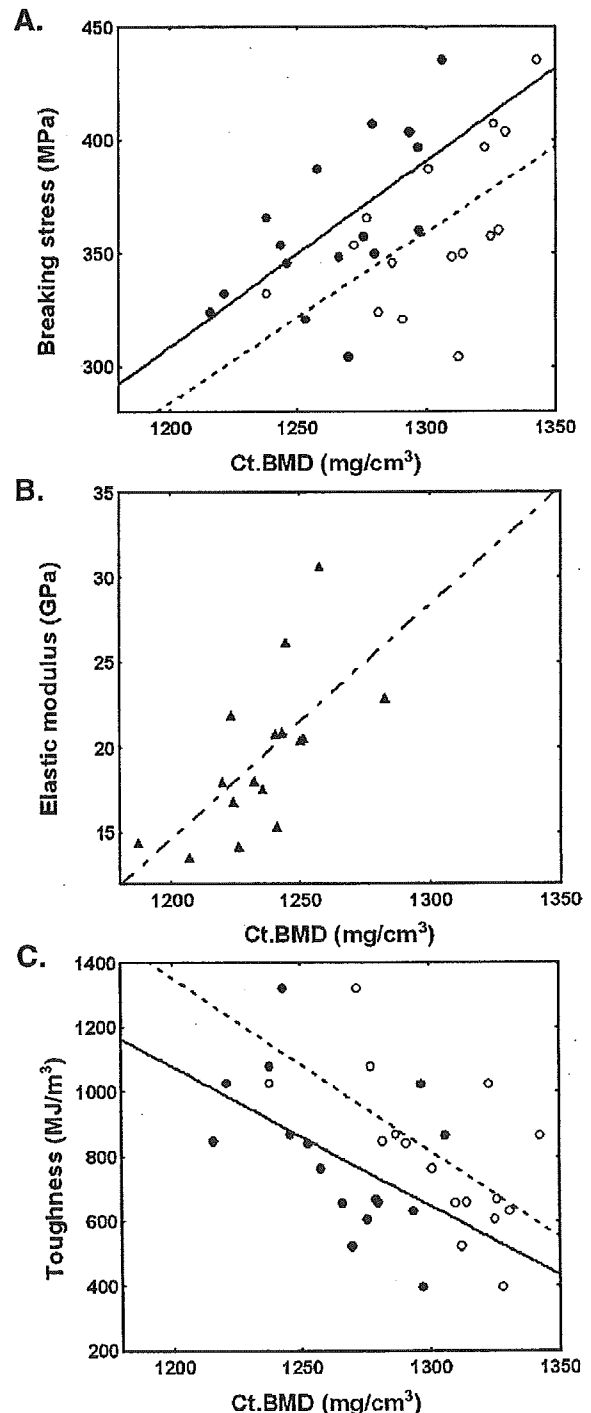


Fig. 2. The significant correlations of material properties to cortical bone density (Ct.BMD) in Table 5 were graphed. (A) Breaking stress positively correlated with the total-Ct.BMD ($r = 0.630$, $r^2 = 0.397$, $P = 0.009$) and posterior-Ct.BMD ($r = -0.579$, $r^2 = 0.335$, $P = 0.019$). A backward stepwise multiple regression analysis revealed that a best-fit model to breaking stress included posterior-Ct.BMD and age ($R = 0.784$, $R^2 = 0.615$, $P = 0.002$). (B) Elastic modulus positively correlated with anterior-Ct.BMD ($r = 0.659$, $r^2 = 0.435$, $P = 0.005$). The result of a backward stepwise multiple regression analysis for elastic modulus was the same as that of simple regression analysis. (C) Toughness negatively correlated with total-Ct.BMD ($r = -0.626$, $r^2 = 0.500$, $P = 0.049$) and posterior-Ct.BMD ($r = -0.626$, $r^2 = 0.392$, $P = 0.010$). A backward stepwise multiple regression analysis indicated a best-fit model to toughness, including total-Ct.BMD and age ($R = 0.763$, $R^2 = 0.582$, $P = 0.003$). Solid, dotted, and dashed lines are linear regression lines of material properties. Solid line and closed circle, total-Ct.BMD; dotted line and open circle, posterior-Ct.BMD; dashed line and closed triangle, anterior-Ct.BMD.

Table 6
Final models of backward stepwise multiple linear regression analyses to predict material properties

Dependent variables	Independent variables	Standardized regression coefficient	P value	R ²
Breaking stress	Posterior-Ct.BMD	0.602	0.002	0.615
	Age	-0.530	0.004	
Toughness	Total-Ct.BMD	-0.640	0.009	0.582
	Age	-0.593	0.003	
			0.004	

Ct.BMD, cortical bone mineral density. Initial models for backward stepwise multiple regression analyses included all Ct.BMDs of three different regions, age, body weight, and bone length. The result of the final model to predict elastic modulus was the same as that of simple regression analysis (Table 4). *n* = 16.

with Ct.BMD. In the anterior region, however, there were no significant correlations.

Discussion

We demonstrated a clear difference in Ct.BMD between the anterior and posterior regions using pQCT, which can analyze subregions within the same cross-section (Table 3). The posterior region, with a higher Ct.BMD, was mainly occupied by interstitial bone, which is highly mineralized, with a few small osteons. In contrast, the anterior region had low Ct.BMD due to an increased number of active osteons. Therefore, the assessment of material properties in bone using Ct.BMD should take the heterogeneity of tissue structure into account, even in the same cross-section.

We also demonstrated that this new analytical method for distinguishing the anterior and posterior quadrants in the cortex can predict the changes in material property. Anterior-Ct.BMD was correlated with elastic modulus, and both total- and posterior-Ct.BMD were correlated with breaking stress and toughness (Table 5 and Fig. 2). We think that the anterior cortex is easily deformed due to the less mineralized bone, which is occupied mainly by osteons, and the posterior cortex is brittle due to highly mineralized bone, which is occupied mainly by interstitial bone. Structural mechanical testing is usually performed based on the assumption that bone material is homogeneous. Material strength under bending conditions, however, should depend on both the anterior (tensile) and posterior (compressive) cortex properties. In the present study, loading direction was set such that the maximum tensile stress was induced at the anterior cortex and the maximum compressive stress at the posterior cortex, considering the strain distribution in tibial diaphysis during the voluntary movement of Macaque fascicularis. The strain distribution in Macaque fascicularis might be similar to that of Macaque mulatta [32] because of their similar postures. A backward stepwise analysis suggested that the posterior cortex is important for resisting mechanical loading. During the bending test, fracture is first initiated at the maximum stress (breaking stress), and then the crack travels through the bone to reach the fracture. In the present study, the anterior cortex with a lower Ct.BMD reflected

the characteristics of the elastic part before the bone was broken, and the posterior cortex with a higher Ct.BMD reflected the characteristics after the elastic part (i.e., plastic part) through the breaking point until the fracture. Changes in the material properties at the tibial diaphysis can be monitored by anterior-, posterior-, or total-Ct.BMD, respectively. According to Turner et al. [29], share stress causes 10 to 15 % of the measured deformation in bending tests of whole rodent bones. Although monkey tibiae are not rodent bones (bone structure of monkey is different from that of rodents based on cortical bone with or without osteons), we acknowledge that our indirect calculation of elastic modulus might be inaccurate.

Our aim was to clarify the relationship between Ct.BMD and toughness. Previous studies reported that the suppression of bone turnover reduced toughness with increased mineralization evaluated by the density fractionation method in dog vertebrae or ribs treated with antiresorptive agents, but Ct.BMD measured by pQCT did not change [21,31]. Another investigator reported that Ct.BMD measured by QCT did not reflect toughness in human femur [20]. The lack of a relationship between Ct.BMD and toughness in these reports might be due to the use of Ct.BMD calculated from the whole cortical area based on the assumption that whole cortical tissue is homogeneous. In the present study, we measured regional Ct.BMD in the anterior and posterior quadrant cortices using a new analytic technique segmenting the cross-section with pQCT and demonstrated that total- and posterior-Ct.BMD negatively correlated to toughness. We also demonstrated that toughness positively correlated with osteon-related parameters, such as %On.Ar and %On.B.Ar (Table 5). Our osteon-related results of bone histomorphometry can be used as parameters to assess the degree of mineralization

Table 7
Correlation of cortical bone mineral density with histomorphometric parameters in the left tibial diaphyses

	Anterior-Ct.BMD (<i>n</i> = 17)	Posterior-Ct.BMD (<i>n</i> = 17)
<i>Anterior region</i>		
On.Dn	-0.459 (0.211)	
%On.Ar	-0.332 (0.110)	
%On.B.Ar	-0.321 (0.103)	
%Il.On.Ar	-0.267 (0.071)	
%Sd.On.Ar	-0.330 (0.109)	
Po	-0.452 (0.205)	
%O.Ar ^f	0.229 (0.053)	
<i>Posterior region</i>		
On.Dn		-0.468 (0.219)
%On.Ar		-0.540 (0.292)*
%On.B.Ar		-0.526 (0.277)*
%Il.On.Ar		-0.512 (0.262)*
%Sd.On.Ar		-0.374 (0.140)
Po		-0.232 (0.054)
%O.Ar		0.072 (0.005)

Ct.BMD, cortical bone mineral density; On.Dn, osteon population density; %On.Ar, percent osteonal area; %On.B.Ar, percent osteonal bone area; %Il.On.Ar, percent osteonal area of initial remodeling; %Sd.On.Ar, percent osteonal area of secondary remodeling; Po, porosity; %O.Ar, percent osteoid area. Asterisk shows significant correlation (level of significance: *P* < 0.05). Parentheses: coefficient of determination (*r*²).

because On.Dn was negatively correlated with the degree of mineralization, as reported elsewhere [26,33]. The higher values of the osteon-related parameters reflect the lower degree of mineralization, and the lower values reflect the higher degree of mineralization. Therefore, our findings suggest that posterior-Ct.BMD is a better indicator of the impaired toughness associated with the increased degree of mineralization. The multiple regression model indicated that total-Ct.BMD contributed to toughness more than posterior-Ct.BMD if the effect of age was taken into account. The effect of age might reflect the characteristics of osteonal structure in the anterior cortex in which the enlargement of microdamage might be stopped and/or deflected due to cement lines [24,25]. The positive correlation of %Sd.On.Ar to toughness suggests that the increased number of osteons of secondary remodeling in the posterior cortex improves toughness. The osteons of secondary remodeling in the posterior cortex might be more likely to affect toughness because the area occupied by osteons was lower in the posterior cortex.

Breaking stress was independent of the osteon-related parameters (Table 7), which were negatively related to the degree of mineralization. Factors other than the degree of mineralization might also affect bone material strength. One factor to be considered is the organic matrix, most of which is type I collagen. Because collagen maturity (cross-linking) influences material strength in bone [34], factors regarding collagen production and function might affect breaking stress in this study.

Recently, several studies utilizing pQCT technology were performed in human tibia [35–37]. The distribution of mineralization in bone tissue changes as a consequence of treatment with antiresorptive and anabolic agents [38–40]. Our new analytic method, which distinguishes subregions of cortical bone, might be useful for detecting such slight changes at the tissue level in the same cross-section of bone. This analysis might also be useful to predict the fracture risk of bones and to contribute to reductions in the incidence of fracture.

In conclusion, clear differences in Ct.BMD between the anterior and posterior regions were revealed through the discriminating function of pQCT, based on the fact that the structure of bone tissue is heterogeneous. Posterior-Ct.BMD and total-Ct.BMD were the best variables for predicting breaking stress and toughness, respectively, when age is taken into account. Anterior-Ct.BMD was the best predictor for elastic modulus. The regional distinctions in Ct.BMD are useful to separately predict alterations in the material properties at the tibial diaphysis of the *Cynomolgus* monkey.

Acknowledgments

The authors wish to thank Dr. Bobby John Varghese for his assistance with the English of the manuscript.

References

- [1] Ferretti JL, Capozza RF, Zanchetta JR. Mechanical validation of a tomographic (pQCT) index for noninvasive estimation of rat femur bending strength. *Bone* 1996;18:97–102.
- [2] Ferretti JL. Peripheral quantitative computed tomography (pQCT) for evaluating structural and mechanical properties of small bone. In: An YH, Draughn RA, editors. *Mechanical testing of bone and the bone–implant interface*. Boca Raton, FL: CRC Press; 2000. p. 385–405.
- [3] Ferretti JL. Noninvasive analysis of bone mass, structure, and strength. In: An YH, editor. *Orthopaedic issues in osteoporosis*. Boca Raton, FL: CRC Press; 2002. p. 145–67.
- [4] van der Meulen MC, Jepsen KJ, Mikic B. Understanding bone strength: size isn't everything. *Bone* 2001;29:101–4.
- [5] Danova NA, Colopy SA, Radtke CL, Kalscheur VL, Markel MD, Vanderby R, et al. Degradation of bone structural properties by accumulation and coalescence of microcracks. *Bone* 2003;33:197–205.
- [6] Komatsubara S, Mori S, Mashiba T, Li J, Nonaka K, Kaji Y, et al. Suppressed bone turnover by long-term bisphosphonate treatment accumulates microdamage but maintains intrinsic material properties in cortical bone of dog rib. *J Bone Miner Res* 2004;19:999–1005.
- [7] Rosen HN, Chen V, Cittadini A, Greenspan SL, Douglas PS, Moses AC, et al. Treatment with growth hormone and IGF-I in growing rats increases bone mineral content but not bone mineral density. *J Bone Miner Res* 1995;10:1352–8.
- [8] Lind PM, Lind L, Larsson S, Örborg J. Torsional testing and peripheral quantitative computed tomography in rat humerus. *Bone* 2001;29:265–70.
- [9] Leonard MB, Shults J, Elliott DM, Stallings VA, Zemel BS. Interpretation of whole body dual energy X-ray absorptiometry measures in children: comparison with peripheral quantitative computed tomography. *Bone* 2004;34:1044–52.
- [10] Gorai I, Nonaka K, Kishimoto H, Sakata H, Fujii Y, Fujita T. Cut-off values determined for vertebral fracture by peripheral quantitative computed tomography in Japanese women. *Osteoporos Int* 2001;12:741–8.
- [11] Schoenau E, Neu CM, Rauch F, Manz F. Gender-specific pubertal changes in volumetric cortical bone mineral density at the proximal radius. *Bone* 2002;31:110–3.
- [12] Ferretti JL, Gaffuri O, Capozza R, Cointy G, Bozzini C, Olivera M, et al. Dexamethasone effects on mechanical, geometric and densitometric properties of rat femur diaphyses as described by peripheral quantitative computerized tomography and bending tests. *Bone* 1995;16:119–24.
- [13] Wachter NJ, Krischak GD, Mentzel M, Sarakar M, Ebinger T, Kinzl L, et al. Correlation of bone mineral density with strength and microstructural parameters of cortical bone in vitro. *Bone* 2002;31:90–5.
- [14] Black DM, Cummings SR, Karpf DB, Cauley JA, Thompson DE, Nevitt MC, et al. Randomised trial of effect of alendronate on risk of fracture in women with existing vertebral fractures: Fracture Intervention Trial research group. *Lancet* 1996;348:1535–41.
- [15] Reginster J, Minne HW, Sorensen OH, Hooper M, Roux C, Brandi ML, et al. Randomized trial of the effects of risedronate on vertebral fractures in women with established postmenopausal osteoporosis. Vertebral Efficacy with Risedronate Therapy (VERT) Study Group. *Osteoporos Int* 2000;11:83–91.
- [16] Ettinger B, Black DM, Mitalk BH, Knickerbocker RK, Nickelsen T, Genant HK, et al. Cummings SR for the Multiple Outcomes of Raloxifene Evaluation (MORE) Investigators. Reduction of vertebral fracture risk in postmenopausal women with osteoporosis treated with raloxifene. *JAMA* 1999;282:637–45.
- [17] Zioupos P, Currey JD. Changes in the stiffness, strength and toughness of human cortical bone with age. *Bone* 1998;22:57–66.
- [18] Currey JD, Brear K, Zioupos P. The effects of ageing and changes in mineral content in degrading the toughness of human femora. *J Biomech* 1996;29:257–60.
- [19] Yeni YN, Brown CU, Norman TL. The influence of bone composition and apparent density on fracture toughness of the human femur and tibia. *Bone* 1998;22:79–84.
- [20] Wang XD, Masilamani NS, Mabrey JD, Alder ME, Agrawal CM. Changes in the fracture toughness of bone may not be reflected in its mineral density, porosity, and tensile properties. *Bone* 1998;23:67–72.
- [21] Burr DB, Miller L, Grynpas M, Li J, Boyde A, Mashiba T, et al. Tissue mineralization is increased followed 1-year treatment with doses of bisphosphonate in dogs. *Bone* 2003;33:960–9.

- [22] Bell KL, Loveridge N, Jordan GR, Power J, Constant CR, Reeve J. A novel mechanism or induction of increased cortical porosity in cases of intracapsular hip fracture. *Bone* 2000;27:297–304.
- [23] Mori S, Burr DB. Increased intracortical remodeling following fatigue damage. *Bone* 1993;14:103–9.
- [24] Burr DB, Turner CH, Naick P, Forwood MR, Ambrosius W, Hasan MS, et al. Does microdamage accumulation affect the mechanical properties of bone? *J Biomech* 1998;31:337–45.
- [25] Griffin LV, Gibeling JC, Martin RB, Gibson VA, Stover SM. Model of flexural fatigue damage accumulation for cortical bone. *J Orthop Res* 1997;15:607–14.
- [26] Skedros JG, Sybrowsky CL, Parry TR, Bloebaum RD. Regional differences in cortical bone organization and microdamage prevalence in Rocky Mountain mule deer. *Anat Rec* 2003;274A:837–50.
- [27] Havill LM. Osteon remodeling dynamics in *Macaca mulatta*: normal variation with regard to age, sex, and skeletal maturity. *Calcif Tissue Int* 2004;74:95–102.
- [28] Parfitt AM, Drezner MK, Glorieux MK, Kanis FH, Malluche JA, Meunier PJ, et al. Bone histomorphometry: standardization of nomenclature, symbols and units. Report of the ASBMR histomorphometry nomenclature committee. *J Bone Miner Res* 1987;2:595–610.
- [29] Turner CH, Burr DB. Basic biomechanical measurements of bone: a tutorial. *Bone* 1993;14:595–608.
- [30] Lopez MJ, Markel MD. Bending tests of bone. In: An YH, Draughn RA, editors. *Mechanical testing of bone and the bone-implant interface*. Boca Raton, FL: CRC Press; 2000. p. 207–17.
- [31] Mashiba T, Hirano T, Turner CH, Forwood MR, Johnston CC, Burr DB. Suppressed bone turnover by bisphosphonates increase microdamage accumulation and reduce some biomechanical properties in dog rib. *J Bone Miner Res* 2000;15:613–20.
- [32] Demes B, Qin YX, Stern Jr JT, Larson SG, Rubin CT. Patterns of strain in the Macaque tibia during functional activity. *Am J Phys Anthropol* 2001;116:257–65.
- [33] Yeni YN, Brown CU, Wang Z, Norman TL. The influence of bone morphology on fracture toughness of the human femur and tibia. *Bone* 1997;21:453–9.
- [34] Bonucci E. Basic composition and structure of bone. In: An YH, Draughn RA, editors. *Mechanical testing of bone and the bone-implant interface*. Boca Raton, FL: CRC Press; 2000. p. 3–21.
- [35] Russo CR, Lauretani F, Bandinelli S, Bartali B, Di Iorio A, Volpato S, et al. Aging bone in men and women: beyond changes in bone mineral density. *Osteoporos Int* 2003;14:531–8.
- [36] Moyer-Mileur L, Xie B, Ball S, Bainbridge C, Stadler D, Jee WS. Predictors of bone mass by peripheral quantitative computed tomography in early adolescent girls. *J Clin Densitom* 2001;4:313–23.
- [37] Wosje KS, Binkley TL, Specker BL. Comparison of bone parameters by dual-energy X-ray absorptiometry and peripheral quantitative computed tomography in Hutterite vs. non-Hutterite women aged 35–60 years. *Bone* 2001;29:192–7.
- [38] Sato M, Westmore M, Clendenon J, Smith S, Hannum B, Zeng GQ, et al. Three-dimensional modeling of the effects of parathyroid hormone on bone distribution in lumbar vertebrae of ovariectomized Cynomolgus macaques. *Osteoporos Int* 2000;11:871–80.
- [39] Boivin GY, Chavassieux PM, Santora AC, Yates J, Meunier PJ. Alendronate increases bone strength by increasing the mean degree of mineralization of bone tissue in osteoporotic women. *Bone* 2000;27:687–94.
- [40] Burr DB, Hirano T, Turner CH, Hotchkiss C, Brommage R, Hock JM. Intermittently administered human parathyroid hormone (1–34) treatment increases intracortical bone turnover and porosity without reducing bone strength in the humerus of ovariectomized Cynomolgus monkeys. *J Bone Miner Res* 2001;16:157–65.

Echocardiographic Diagnosis of Muscular Ventricular Septal Defect in a Cynomolgus Monkey (*Macaca fascicularis*)

HIROSHI KOIE, DVM, PHD,^{1*} NAOHIDE AGEYAMA, DVM,² FUMIKO ONO, DVM, PHD,³
KIICHI KANAYAMA, DVM, PHD,¹ TAKEO SAKAI, DVM, PHD,¹
AND TADASHI SANKAI, DVM, PHD²

There have been only a few case reports of heart disease in monkeys. In the case we present, a cardiac murmur was auscultated in a 26-month-old male cynomolgus monkey during a routine physical examination. Echocardiography of this monkey revealed features indicating blood flow from the left ventricle to the right ventricle through the ventricular septum. These findings clarified that the animal had a muscular interventricular septal defect.

Case Report

Antemortem detection of cardiac disease in laboratory nonhuman primates is rare. In particular, only a few nonhuman primate species have been documented to have ventricular septal defects (VSD). Cook and colleagues identified a cardiac murmur in a male orangutan during vasectomy and predicted the presence of a left-right shunt in light of high oxygen saturation in the right ventricle as detected by cardiac catheterization (2). Binhazim and coworkers performed echocardiography in a newborn chimpanzee, suspected the presence of VSD, and finally confirmed the presence of a hole in the membranous ventricular septum through postmortem examination (1). Swindle and colleagues reported the initial case of VSD diagnosed antemortem by using two-dimensional echocardiography and cardiac catheterization in a male rhesus macaque; the authors confirmed the presence of a defective hole in the membranous ventricular septum (5).

Our case report involves a cynomolgus macaque (*Macaca fascicularis*) in which a cardiac murmur was auscultated during a routine physical examination. The Tsukuba Primate Research Center maintains and keeps approximately 1400 cynomolgus monkeys in a closed environment for biomedical research. These macaques are used for numerous research projects at our institution, including vaccinology, infectious disease, gene therapy, regenerative medicine, and aging studies. To the best of our knowledge, this is the first report of muscular VSD in a cynomolgus macaque.

The animal was a 26-month-old male cynomolgus monkey (body weight, 2.1 kg) that underwent a thorough examination of the circulatory organs after the detection of a cardiac murmur. The murmur (Levine IV/VI) was heard with a point of maximum intensity in the right anterior chest. Electrocardiography revealed a low potential in all leads (R wave, 0.33 mV; S wave, 0.15 mV; lead II; Fig. 1). When the heart was viewed by radiography, the cranial waist was lost in the lateral view (Fig. 2). The cranial waist is the angle formed between the trachea and heart base. When it disappears in dog and cat, right heart enlargement is suspected. Because of the young age of this monkey, a prominent thymus must also be considered as a cause of the lack of cardiac waist.

Echocardiography (Pro Sound SSD-5000, Aloka, Tokyo, Japan) was

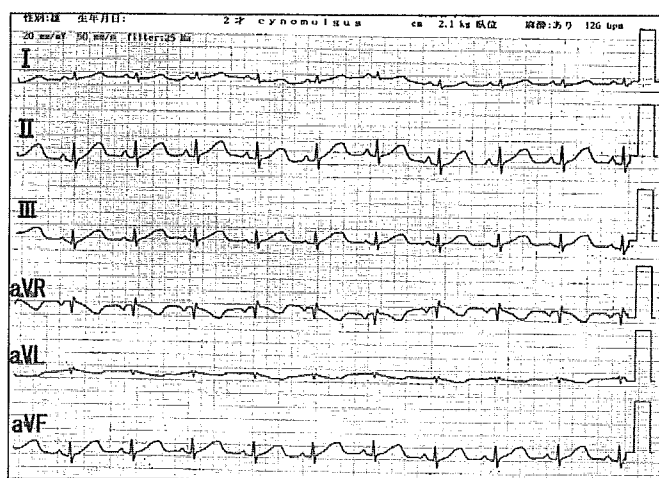


Figure 1. Electrocardiography detected a low potential in all leads (R wave, 0.33 mV; S wave, 0.15 mV; lead II). 1 cm = 1 mV, 50 mm/sec.

performed using the right parasternal approach, and blood inflow into the right ventricle through the muscular part of the ventricular septum, as well as turbulent flow, were observed in the short-axis view (Fig. 3). The blood flow rate was measured to be 5.0 m/sec (pressure gradient, 100 mm Hg) by the continuous-wave Doppler method. In addition, retraction of the same region was observed on the right ventricular side of the septum during the systolic phase in the long-axis view (Fig. 4). In light of these echocardiograms and the young age of the animal, this macaque was diagnosed with congenital muscular VSD. The plasma concentration of atrial natriuretic peptide (33.3 pg/ml), which is secreted by atrial muscle cells and used as an index of heart failure in humans, was within the normal range (4). Results of a complete blood cell and serum chemistry tests were all within normal limits.

Discussion

In humans, the development of VSD likely is due to genetic mutation, and association with a frameshift mutation of *GATA4* has been suggested (3). In monkeys, no involvement of any gene has been documented, but association with gene mutation is expected to be a cause, similar to that in humans. Accordingly, it may be important to further investigate the potential for genetic involvement of VSD in monkeys.

As described earlier, there have been very few reports of the antemortem diagnosis of VSD in monkeys, and none reported in

Department of Veterinary Medicine, College of Bioresource Sciences, Nihon University, 1866 Kameino Fujisawa, Kanagawa, 252-8510 Japan¹; Tsukuba Primate Research Center, National Institute of Biomedical Innovation, Hachimandai 1, Tsukuba, Ibaraki, 305-0843 Japan²; The Corporation for Production and Research of Laboratory Primates, Hachimandai 1, Tsukuba, Ibaraki, 305-0843 Japan³.

*Corresponding author.

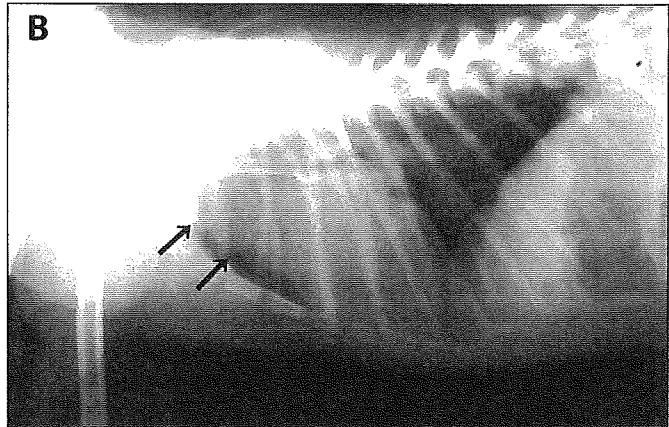
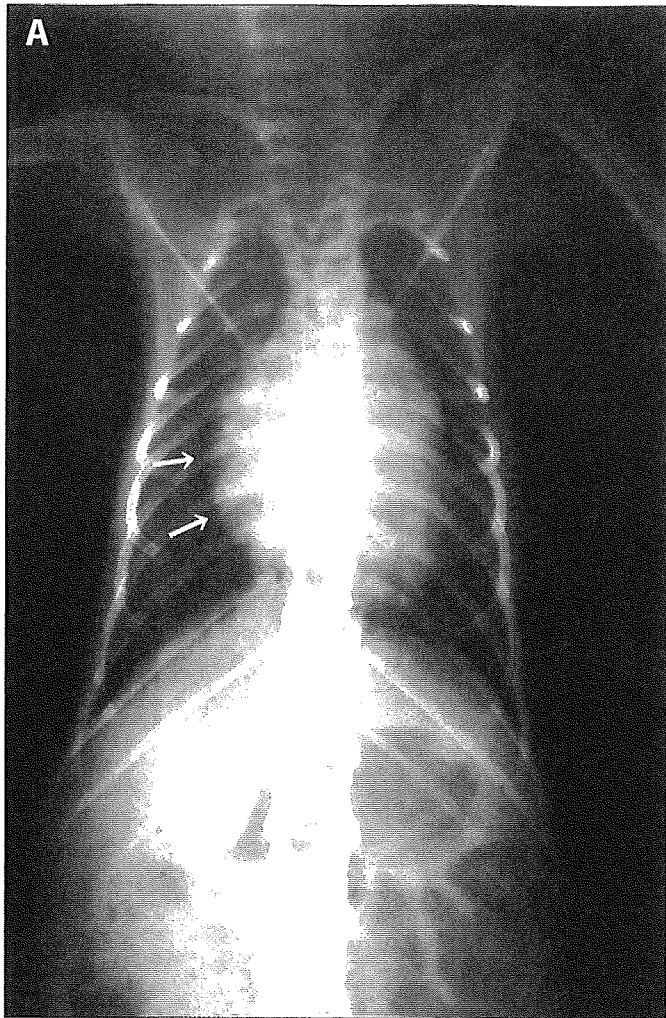


Figure 2. Chest radiography (A, ventrodorsal view; B, lateral view). The cranial waist was lost in the lateral view (B, arrows). Note the right heart expansion (A, arrows).

cynomolgus monkeys. Over a 4-year period of time, Swindle and colleagues surveyed one rhesus monkey in which VSD was diagnosed antemortem. This animal sired seven offspring, but none of the newborns exhibited features of VSD. These investigators also used echocardiography to evaluate the parents of the monkey with VSD, but no abnormalities were identified (5).

The VSD noted in our cynomolgus monkey is the first documented case of muscular VSD in nonhuman primates. Only membranous VSD previously has been reported in monkeys (1, 2, 5). In addition, the presented case is the first in monkeys in which the pressure gradient between the left and right intraventricular pressures was measured using echocardiographic Doppler. Pressure gradient is a very important test

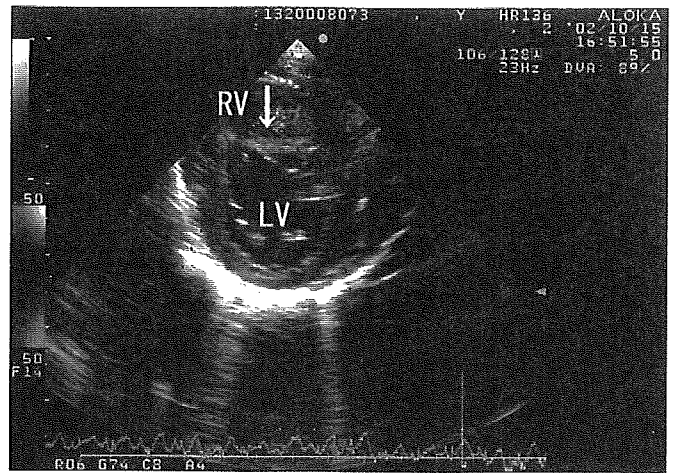


Figure 3. Turbulent blood inflow into the right ventricle through the muscular part of the ventricular septum (arrow) was observed in the short-axis view by the right parasternal approach. The abnormal blood flow rate was 5.0 m/sec (pressure gradient, 100 mm Hg) between the left and right ventricles through the defect hole. LV, left ventricle; RV, right ventricle.

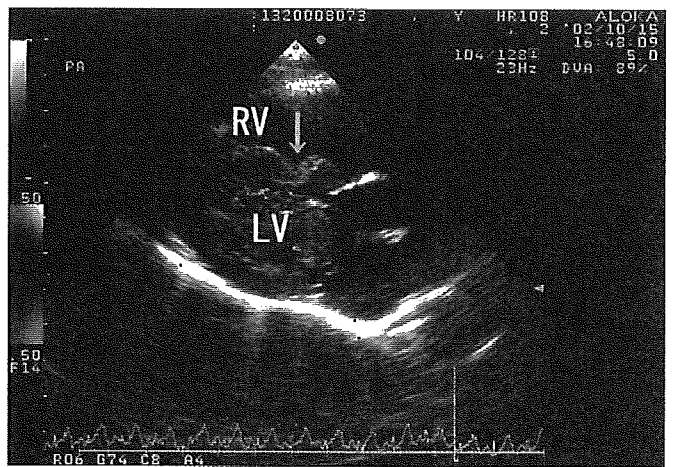


Figure 4. Left ventricular long-axis view. Collapse of the same region highlighted in Fig. 3 (arrow) occurred during the systolic phase. LV, left ventricle; RV, right ventricle.

item for prediction of the prognosis of VSD. The normal difference between left and right intraventricular pressures is about 100 mm Hg. In this animal, the pressure gradient was 100 mm Hg, clarifying that normal intraventricular pressure was maintained despite blood flow between the left and right ventricles. As supportive findings, there were no thickening of the right ventricular wall and no right ventricular dilation, which are characteristic for right ventricular hypertension.

As described earlier, echocardiography may be used as an important method for the diagnosis and prognosis of cardiac diseases in nonhuman primates. As of the time of this report, the animal is 4 years of age and is still under observation with no current clinical symptoms of cardiac disease. We predict that this animal may develop clinical symptoms, such as exercise intolerance, as it ages. Continued monitoring of the disease course in this animal likely will provide important information for analysis of VSD in cynomolgus monkeys.

Acknowledgments

This research was supported by a Nihon University Individual Research Grant for 2003.

References

1. Bin hazim, A. A., P. Alford, and M. Miller. 1994. Ventricular septal defect in an infant chimpanzee (*Pan troglodytes*). *J. Med. Primatol.* 23:362-364.

2. Cook, R. A., P. Sheppardson, M. McGinn, M. L. Roskop, and B. Y. Wong. 1986. Evaluation of a ventricular septal defect in an orangutan: a case report. *J. Med. Primatol.* **15**:303-308.
3. Garg, V., I. S. Kathiriyai, R. Barnes, M. K. Schluterman, I. N. King, C. A. Butler, C. R. Rothrock, R. S. Eapen, K. Hirayama-Yamada, K. Joo, R. Matsuoka, J. C. Cohen, and D. Srivastava. 2003. GATA4 mutations cause human congenital heart defects and reveal an interaction with TBX5. *Nature* **424**:443-447.
4. Raine, A. E. G., D. Phil, P. Erne, E. Buergisser, F. B. Mueller, P. Bolli, F. Burkart, and F. R. Buchler. 1986. Atrial natriuretic peptide and atrial pressure in patients with congestive heart failure. *N. Engl. J. Med.* **315**:533-537.
5. Swindle, M. M., J. S. Kan, R. J. Adams, F. L. Starr, III, M. A. Samphilipo, Jr., and W. P. Porter. 1986. Ventricular septal defect in a rhesus monkey. *Lab. Anim. Sci.* **36**:693-695.

Safe And Efficient Collection of Cytokine-Mobilized Peripheral Blood Cells From Cynomolgus Monkeys (*Macaca fascicularis*) with Human Newborn-Equivalent Body Weights

Naohide AGEYAMA^{1, 2)}, Yutaka HANAZONO³⁾, Hiroaki SHIBATA^{1, 3)}, Fumiko ONO²⁾, Hiromi OGAWA²⁾, Takeyuki NAGASHIMA⁴⁾, Yasuji UEDA⁴⁾, Yasuhiro YOSHIKAWA⁵⁾, Mamoru HASEGAWA⁴⁾, Keiya OZAWA³⁾, and Keiji TERAO¹⁾

¹⁾Tsukuba Primate Research Center, National Institute of Biomedical Innovation, Ibaraki 305-0843,

²⁾Corporation for Production and Research of Laboratory Primates, Ibaraki 305-0843, ³⁾Center for Molecular Medicine, Jichi Medical School, Tochigi 329-0498, ⁴⁾DNAVEC Corporation, Ibaraki 305-0856, ⁵⁾Department of Biomedical Science, Graduate School of Agriculture and Life Science, University of Tokyo, Tokyo 113-8657, Japan

Abstract: Hematopoietic stem cells in bone marrow can be mobilized into peripheral blood by cytokine administration. Cytokine-mobilized peripheral blood stem cells are of great use in clinical applications. We previously established a modified procedure for the collection of cytokine-mobilized peripheral blood cells from rhesus monkeys (*Macaca mulata*) using a commercially available apparatus originally developed for human subjects. In this study, we examined the efficacy and safety of this method with even smaller macaques, cynomolgus monkeys (*Macaca fascicularis*), which are equivalent to human newborns in body weight (mean = 3.3 kg). Using the manufacturer's unmodified protocol (n=6), one monkey died of cardiac failure and three developed severe anemia. In contrast, using our modified procedure (n=6), no such complication was observed in any animal. In addition, the harvested nuclear cell, mononuclear cell and CD34⁺ cell counts were significantly higher with the modified method. The modified method should allow safe and efficient collection of cytokine-mobilized peripheral blood cells from non-human primates as small as human newborns in a non-invasive manner.

Key words: cynomolgus monkey, cytokine mobilization, leukapheresis, peripheral blood stem cell

Introduction

Although hematopoietic stem cells (HSCs) usually reside in the bone marrow, they can be mobilized into

the peripheral blood by the administration of cytokines such as granulocyte colony-stimulating factor (G-CSF) [24]. Cytokine-mobilized peripheral blood stem cells are widely used for autologous and allogeneic trans-

(Received 23 April 2005 / Accepted 21 July 2005)

Address corresponding: Y. Hanazono, Division of Regenerative Medicine, Center for Molecular Medicine, Jichi Medical School, 3311-1 Yakushiji, Minamikawachi, Tochigi 329-0498, Japan

Table 1. Hematological analysis of cynomolgus monkeys after cytokine treatment

Animals	Sex	Age (years)	Body weight (kg)	After cytokine treatment				
				White blood cells (10 ² /μl)	Red blood cells (10 ⁴ /μl)	Hemoglobin (g/dl)	Hematocrit (%)	Platelets (10 ⁴ /μl)
Unmodified procedure								
292049	Male	6	4.6	680	632	12.0	41.4	36.1
293051	Female	6	2.5	1091	535	10.7	39.0	35.7
292079	Female	7	3.2	514	480	11.6	36.5	35.8
292238	Female	7	3.2	548	653	13.4	44.4	30.0
394029	Female	5	3.2	355	590	11.7	42.3	42.4
296116	Male	3	3.1	361	583	12.0	43.8	26.6
Average		5.7	3.3	592	579	11.9	41.2	34.4
Modified procedure								
001046	Female	3	3.5	872	484	12.4	38.9	43.7
001045	Male	3	3.3	519	415	9.7	33.4	44.2
001049	Male	3	3.5	434	501	12.3	38.7	43.8
001053	Male	3	2.6	802	456	10.3	35.1	57.7
001047	Male	4	3.3	805	438	11.1	35.3	40.4
398042	Male	5	3.8	887	521	11.9	36.8	38.4
Average		3.5	3.3	720	469	11.3	36.3	44.7

plantation therapies to treat hematological malignancies such as leukemia and lymphoma [16, 17]. The cells have also been intensively studied as a donor source of stem cells for gene and cell therapies [11, 20, 30]. An efficient method for collecting cytokine-mobilized peripheral blood cells in monkeys would facilitate such studies in a clinically relevant manner.

The procedure for collecting peripheral blood cells from living animals is referred to as leukapheresis: peripheral blood is withdrawn, nuclear cells are removed, and the rest of the blood is returned [7]. Automatic instruments for this procedure are commercially available [23, 27]. The removed cells are then enriched for a stem cell fraction such as CD34⁺ or AC133⁺ cells for clinical applications [5, 29]. Although leukapheresis is widely conducted for human adults, it is difficult to apply to regular experimental macaque monkeys because of their small size. Generally speaking, the procedures involved preclude the application of leukapheresis to animals weighing less than 10 kg in body weight [18].

We and others have previously reported leukapheresis procedures for non-human primates with body weights of less than 10 kg using rhesus monkeys (*Macaca mulata*, average 7 kg) [3, 9]. In such small animals, acute cardiac failure due to the relatively large extracorporeal blood flow is a critical adverse event which

can occur during leukapheresis. To avoid this, we modified the procedure by reducing the extracorporeal blood volume as much as possible and adjusting the withdrawal speed frequently in response to the results of real-time monitoring of hemoglobin (Hb) and hematocrit (Ht) values [3]. In this study, we examined the efficacy and safety of our procedure using even smaller non-human primates, cynomolgus monkeys (*Macaca fascicularis*, average 3.3 kg), which have body weights equivalent to human newborns.

Materials and Methods

Animals

Twelve cynomolgus monkeys (*Macaca fascicularis*) (3–7 years old, 2.5–4.6 kg) bred at the Tsukuba Primate Research Center (Ibaraki, Japan) were enrolled in this study (Table 1). Animals were free of intestinal parasites, herpes-B, simian type-D retrovirus and simian varicella virus. All monkeys were housed indoors at 23–27°C and 50–70% humidity with 12 air changes per hour and a 12-h/12-h light/dark cycle. Animals were individually housed in stainless steel cages and fed 70 g of commercial monkey chow (Type AS; Oriental Yeast, Chiba, Japan) and 200 g of fruit daily. All monkeys were healthy as assessed by annual examinations. This

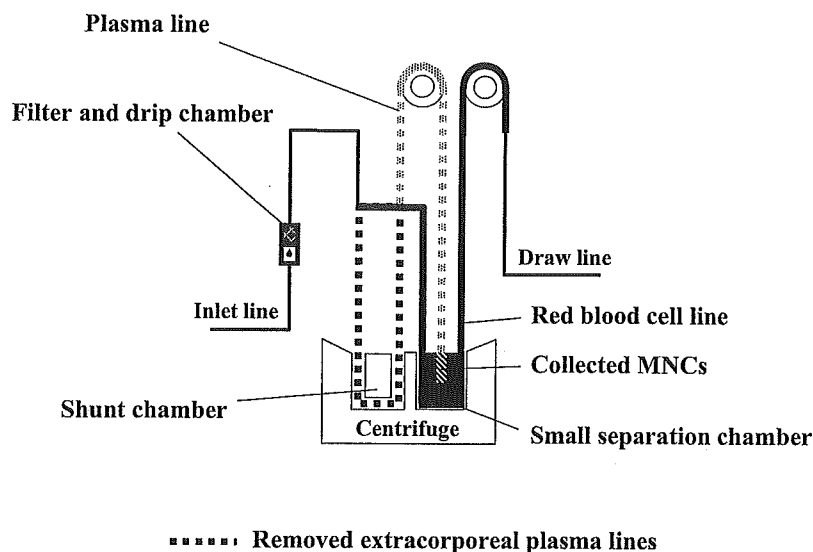


Fig. 1. Diagram of the apheresis kit after the modifications. In the modified system, a small separation chamber (S25A) was installed in the standard apheresis kit and the extracorporeal blood lines were shortened to reduce the extracorporeal blood volume from 130 to 70 ml. MNCs, mononuclear cells.

study was conducted according to the Rules for Animal Care and Management of the Tsukuba Primate Research Center [12] and the Guiding Principles for Animal Experiments Using Non-human Primates formulated by the Primate Society of Japan [21]. This study was approved by the Animal Welfare and Animal Care Committee of the National Institute of Infectious Diseases.

Apparatus

A CS3000 blood separator (Baxter, Deerfield, IL, USA) was used as described previously [3]. Briefly, a standard apheresis kit was installed in the CS3000 blood separator. The smallest separation chamber (S25A) in the kit was used. To reduce the extracorporeal blood volume, the plasma line of the standard apheresis kit was cut away and the red blood cell (RBC) line was directly connected to the inlet line using a polypropylene tube connector (Iuchi, Osaka, Japan) under sterile conditions, bypassing the shunt chamber (Fig. 1). In addition, the regular inlet and draw lines were replaced with lines shorter in length and smaller in diameter (extension tube, 70 cm, 1.4 ml, 2.5 mm diameter; TOP, Tokyo, Japan) to further reduce the extracorporeal blood volume.

Preparative regimen

During the three weeks preceding leukapheresis, a

total of 60–90 ml of autologous blood was obtained from each monkey as described previously [6]. The collected autologous blood was supplemented with acid citrate dextrose (ACD) and stored at 4°C prior to use. Recombinant human (rh) stem cell factor (SCF, 50 µg/kg; Amgen, Thousand Oaks, CA, USA) and rhG-CSF (50 µg/kg; Chugai, Tokyo, Japan) were administered to animals subcutaneously daily during the 5 days preceding leukapheresis [9]. On the day of leukapheresis, the right or left femoral artery was cannulated using a 5-Fr polyurethane catheter (Anthon PU; Toray, Tokyo, Japan). The saphenous vein was also catheterized with a 19-gauge intracatheter (Terumo, Tokyo, Japan). This cannulation was performed under general anesthesia with the administration of ketamine hydrochloride (Ketalar; Sankyo, Tokyo, Japan).

Leukapheresis

All leukapheresis procedures were performed under general anesthesia with endotracheal intubation (Fig. 2). Vital signs were monitored with electrocardiography, blood pressure, oxygen saturation and respiration. Animals received a dose of 100 U/kg heparin (Aventis Pharma, Frankfurt, Germany) just before the initiation of leukapheresis. The plasma flowed directly into the inlet line bypassing the shunt chamber (Fig. 1). The inlet line

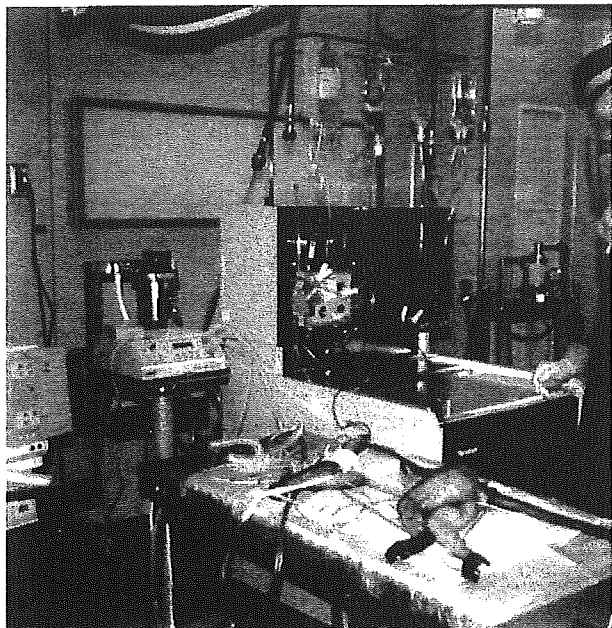


Fig. 2. Leukapheresis procedure. Cynomolgus monkeys were intubated and all procedures were performed under general anesthesia with monitoring of vital signs. The body weights (3.3 kg on average, see Table 1) were similar to those of human newborns.

was connected to an intracatheter placed in the saphenous vein of the animal. The draw line was connected to a catheter in the femoral artery just before starting the procedure. The apheresis kit was filled with the autologous blood collected as described above.

After the leukapheresis was completed, the blood remaining in the apheresis kit was recovered and either used to fill another apheresis kit or returned into the animal. Immediately after the leukapheresis, animals were given an appropriate dose (10 mg per 1,000 U heparin) of protamine sulfate (Aventis Pharma) to neutralize heparin. Animals also received a course of 0.5 mg/kg butorphanol tartrate (Bristol-Myers Squibb, New York, NY, USA) intramuscularly for 3 days to alleviate any post-operative pain.

Analysis of leukapheresis products

The product obtained during leukapheresis was collected in the S25A separation chamber. The product (40–45 ml) was mixed with 7 ml of ACD. The recovered RBCs, white blood cells (WBCs), mononuclear cells and platelets were enumerated with a Sysmex K-4500 instrument (Toa-iyoudenshi, Kobe, Japan). Hb

and Ht values were also examined with this instrument. Although the instrument was originally developed for human blood samples, we have confirmed that it works properly for monkey blood samples. Blood cells were collected after centrifugation at 1,200 rpm for 10 min and suspended in the ACK buffer (Biosource, Camarillo, CA, USA) for the lysis of RBCs. CD34⁺ cells were isolated with immunomagnetic beads conjugated to a monoclonal antibody clone 561 (DynaL, Lake Success, NY, USA) that reacts to both human and cynomolgus CD34 [26, 33]. The harvested CD34⁺ cells were counted. CD34 is a clinically-relevant cell-surface marker of HSCs, and CD34⁺ cell transplantation is widely performed as HSC transplantation in patients with cancer or other disorders [5, 19].

Results

We examined the safety and efficacy of leukapheresis using the manufacturer's protocol (n=6) and our modified version (n=6) in cynomolgus monkeys (Fig. 2). In both groups, we administered G-CSF and SCF to monkeys for 5 days to mobilize HSCs into the peripheral blood. The administration resulted in an increase in peripheral WBC counts to 66,000 cells/ μ l on average (Table 1), and was not associated with any adverse effect such as fever or anorexia. There was no significant difference in the increase in the peripheral WBC counts after cytokine treatment between the unmodified and modified procedure groups. In the modified protocol, a small separation chamber (S25A) was installed instead of the regular one in the blood separator, and the extracorporeal blood lines in the standard apheresis kit were shortened [3, 9, 22]. As a result, the extracorporeal blood volume was reduced from 130 to 70 ml (Fig. 1). In both groups, blood was processed at a rate of 10–12 ml/min and the total processed volume was two to three times the estimated total blood volume [4] of each animal (Table 2). In the modified protocol, every time the processed blood volume increased by 50 ml/kg, a 1-ml blood sample was collected *via* the draw line, and Hb and Ht values were examined throughout the procedure to adjust the plasma pump speed [14]. The plasma pump speed was increased when Hb and Ht values decreased. Conversely, it was decreased when Hb and Ht values increased. In addition, when Hb and Ht values increased, normal saline

Table 2. Leukapheresis procedures

Animals	Estimated total blood volume (ml)*	Processed blood		Complications
		Total volume (ml)	ml/kg	
Unmodified procedure				
292049	293	600	130	None
293051	217	600	240	Severe anemia
292079	231	400	125	Severe anemia Died of cardiac failure
292238	231	600	188	None
394029	231	700	219	Severe anemia
296116	227	600	194	None
Average	238	583	183	
Modified procedure				
001046	237	750	214	None
001045	236	600	182	None
001049	244	800	229	None
001053	205	500	192	None
001047	236	600	182	None
398042	258	700	183	None
Average	236	658	197	

*The total blood volume was estimated with the following formula [4]. For males, (Total blood volume, ml) = 44.07 × (Body weight, kg) + 90.25. For females, (Total blood volume, ml) = 19.95 × (Body weight, kg) + 167.24.

was infused *via* the inlet line for volume replacement.

After the completion of the unmodified procedure (n=6), one animal died of acute cardiac failure and three animals developed severe anemia (Hb<8.0 g/dl, Fig. 3). In contrast, none of the animals that underwent the modified procedure (n=6) developed cardiac failure or severe anemia (Table 2). The Hb and Ht values were significantly better preserved during the modified procedure (Fig. 3). In addition, the numbers of harvested nuclear cells, mononuclear cells, and CD34⁺ cells were significantly increased with the modified procedure compared to the unmodified one (Fig. 4).

The leukapheresis products were contaminated with considerable amounts of RBCs and platelets, when the apparatus was operated in automatic mode under the unmodified protocol. In the modified version, we performed manual adjustment of the plasma pump speed in response to the results of the real-time monitoring of Hb and Ht values during the leukapheresis as described above, and successfully reduced the contamination (data not shown). The reduction in contaminated RBCs also contributed to the amelioration of anemia after leukapheresis in the modified procedure group. No microbial contamination

was detected in cultures of the leukapheresis products from the unmodified or modified procedures.

Discussion

In this paper, we reported leukapheresis in cynomolgus monkeys. Our modified protocol significantly improved mononuclear and CD34⁺ cell harvest compared to the manufacturer's protocol. Under our modified procedure, we routinely collected 5 × 10⁶ CD34⁺ cells per kg, which is equivalent to numbers in human trials published in the literature [13, 25, 28, 31]. Thus, with our modified protocol, it is possible to collect sufficient numbers of CD34⁺ stem cells for various applications including transplantation experiments in monkeys. In fact, we achieved successful hematopoietic reconstitution in myeloablated cynomolgus monkeys after the autologous transplantation of CD34⁺ cells obtained with this procedure [2]. Of note, this procedure can be safely and effectively applied to monkeys with small body weights (2.6–3.8 kg), equivalent to those of human newborns. Although numerous clinical trials have demonstrated the safety and effectiveness

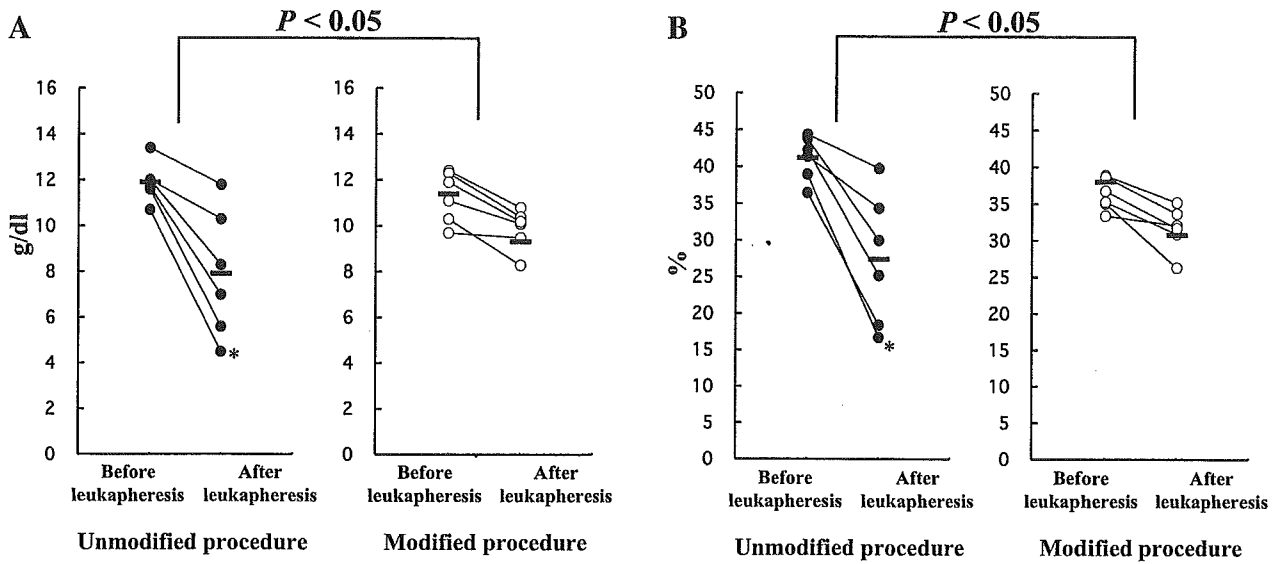


Fig. 3. Avoidance of severe anemia with the modified procedure. The degree of anemia was significantly ameliorated with the modified procedure as compared to the unmodified one as assessed by the ratios of hemoglobin (A) and hematocrit levels (B) after versus before the leukapheresis. One monkey died of cardiac failure (*, 292079) after the unmodified procedure. A: Hemoglobin levels. B: Hematocrit levels.

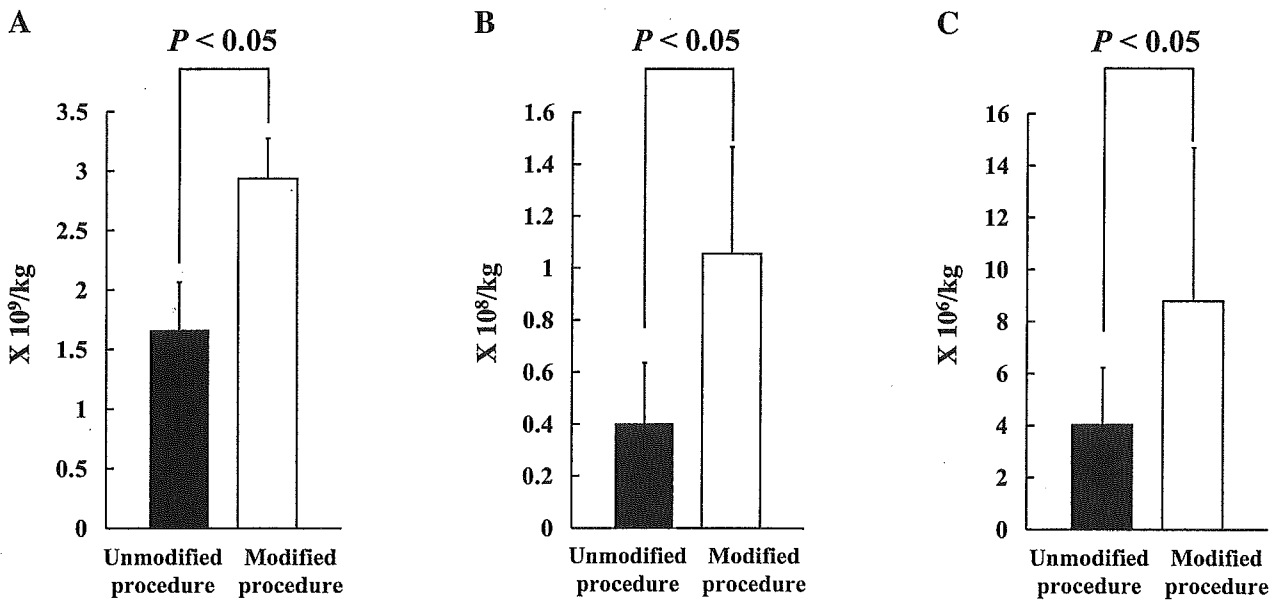


Fig. 4. Larger harvest of cells with the modified procedure. The numbers of harvested nuclear cells (A), mononuclear cells (B), and CD34⁺ cells (C) were significantly increased with the modified procedure. A: Total nuclear cells. B: Mononuclear cells. C: CD34⁺ cells.

of leukapheresis for adults [10, 13, 25, 28] and children [1, 8, 15, 31], only one very limited trial has been conducted on a human newborn baby [32]. To our knowledge, this paper is the first systematic documentation of leukapheresis for small primates.

One of the most serious complications in leukapheresis with small animal subjects is cardiac failure due to the relatively large amount of extracorporeal blood volume [10, 32]. The main symptoms include hypotension and dyspnea, which sometimes result in

death, e.g. animal 292079 (Table 2). To avoid this complication, the extracorporeal blood volume should be reduced as much as possible. No monkeys underwent cardiac failure after our modified procedure. There was, however, an age variation in the unmodified and modified procedure groups. The unmodified procedure group included higher age animals (6 and 7 years). Cynomolgus monkeys of these ages are young adults, and presumably they are more resistant to stress or invasion than monkeys of a juvenile age (3 years). Clearly, the age distribution of the groups, the higher age monkeys belonging to the modified procedure group, was not better than the present way.

Non-human primate models would be useful for pre-clinical studies of cell and gene therapies. We have previously reported the transplant of CD34⁺ stem cells into the ischemic myocardium in cynomolgus monkeys and found that the cardiac function was improved, indicating that further investigation is warranted for clinical application of CD34⁺ stem cell transplant to such disorder [34]. In other studies, we successfully transplanted gene-modified CD34⁺ stem cells into cynomolgus monkeys as a preclinical gene therapy [11, 30]. In this way, our safe and efficient method for collecting peripheral blood stem cells should allow investigators to develop and test new therapies using stem cells in small non-human primates.

Acknowledgments

We are grateful to Masaaki Kimikawa and Kei Eguchi (Department of Surgery III, Tokyo Women's Medical University) for their helpful discussions. We thank Hyato Narita and Katsuhiko Komatsuzaki for their handling and care of the monkeys. We acknowledge Amgen's supply of SCF and Chugai's supply of G-CSF. This study was supported by grants (KAKENHI, HAITEKU, JMS 21st Century COE Program, and Creation of Innovations) from the Ministry of Education, Culture, Sports, Science and Technology of Japan as well as grants (KAKENHI) from the Ministry of Health, Labour and Welfare of Japan.

References

1. Abe, T., Makimoto, A., Kawano, Y., Okamoto, Y., Kajiume, T., Nakagawa, R., Watanabe, H., Sato, J., Watanabe, T., Kuroda, Y., and Takaue, Y. 1998. Intra-apheresis recruitment of blood progenitor cells in children. *Transfusion* 38: 944-950.
2. Ageyama, N., Hanazono, Y., Shibata, H., Ohto, K., Ono, F., Nagashima, T., Ueda, Y., Donahue, R.E., Hasegawa, M., Ozawa, K., Yoshikawa, Y., and Terao, K. 2002. Safe and efficient methods of autologous hematopoietic stem cell transplantation for biomedical research in cynomolgus monkeys. *Comp. Med.* 52: 445-451.
3. Ageyama, N., Kimikawa, M., Eguchi, K., Ono, F., Shibata, H., Yoshikawa, Y., and Terao, K. 2003. Modification of the leukapheresis procedure for use in rhesus monkeys (*Macaca mulata*) *J. Clin. Apher.* 18: 26-31.
4. Ageyama, N., Shibata, H., Narita, H., Hanari, K., Kohno, A., Ono, F., Yoshikawa, Y., and Terao, K. 2001. Specific gravity of whole blood in cynomolgus monkeys (*Macaca fascicularis*), squirrel monkeys (*Saimiri sciureus*) and tamarins (*Saguinus labiatus*) and total blood volume in cynomolgus monkeys. *Contemp. Top. Lab. Anim. Sci.* 40: 33-35.
5. Berenson, R.J., Bensinger, W.I., Hill, R.S., Andrews, R.G., Garcia-Lopez, J., Kalamasz, D.F., Still, B.J., Spitzer, G., Buckner, C.D., Bernstein, I.D., and Thomas, E.D. 1991. Engraftment after infusion of CD34⁺ marrow cells in patients with breast cancer or neuroblastoma. *Blood* 77: 1717-1722.
6. Biesma, D.H., Kraaijenhagen, R.J., Dalmulder, J., Marx, J.J., and van de Wiel, A. 1994. Recombinant human erythropoietin in autologous blood donors: a dose-finding study. *Br. J. Haematol.* 86: 30-35.
7. Blanchette, V.S., McCombie, N.E., and Rock, G. 1985. Factors that influence lymphocyte yields in lymphocytapheresis. *Transfusion* 25: 242-245.
8. Diaz, M.A., Alegre, A., Benito, A., Villa, M., and Madero, L. 1998. Peripheral blood progenitor cell collection by large-volume leukapheresis in low-weight children. *J. Hematother.* 7: 63-68.
9. Donahue, R.E., Kirby, M.R., Metzger, M.E., Agricola, B.A., Sellers, S.E., and Cullis, H.M. 1996. Peripheral blood CD34⁺ cells differ from bone marrow CD34⁺ cells in Thy-1 expression and cell cycle status in nonhuman primates mobilized or not mobilized with granulocyte colony-stimulating factor and/or stem cell factor. *Blood* 87: 1644-1653.
10. Goldberg, S.L., Mangan, K.F., Klumpp, T.R., Macdonald, J.S., Thomas, C., Mullaney, M.T., and Au, F.C. 1995. Complications of peripheral blood stem cell harvesting: review of 554 PBSC leukapheresis. *J. Hematother.* 4: 85-90.
11. Hanazono, Y., Nagashima, T., Takatoku, M., Shibata, H., Ageyama, N., Asano, T., Ueda, Y., Dunbar, C.E., Kume, A., Terao, K., Hasegawa, M., and Ozawa, K. 2002. *In vivo* selective expansion of gene-modified hematopoietic cells in a nonhuman primate model. *Gene Ther.* 9: 1055-1064.
12. Honjo, S. 1985. The Japanese Tsukuba Primate Center for Medical Science (TPC): an outline. *J. Med. Primatol.* 14: 75-89.
13. Jeanne, M., Bouzgarrou, R., Lafarge, X., Fizet, D., Dazey, B., Vezon, G., and Ivanovic, Z. 2003. Comparison of CD34⁺

- cell collection on the CS-3000+ and Amicus blood cell separators. *Transfusion* 43: 1423–1427.
14. Kajiume, T., Kawano, Y., Takaue, Y., Abe, T., Okamoto, Y., Makimoto, A., Watanabe, T., Sato, J., Yokobayashi, A., and Kuroda, Y. 1998. Continuous monitoring of hematocrit values during apheresis for allogeneic peripheral blood stem cell collection. *J. Hematother.* 7: 493–497.
 15. Kanold, J., Halle, P., Rapatel, C., Berger, M., Gembara, P., de Lumley, L., Vannier, J.P., Lutz, P., Plantaz, D., Malpuech, G., and Demeocq, F. 1998. Safe and efficient peripheral blood stem cell collection in the smallest of children. *Ther. Apher.* 2: 49–57.
 16. Kessinger, A., Armitage, J.O., Smith, D.M., Landmark, J.D., Bierman, P.J., and Weisenburger, D.D. 1989. High-dose therapy and autologous peripheral blood stem cell transplantation for patients with lymphoma. *Blood* 74: 1260–1265.
 17. Korbling, M., Przepiorka, D., Huh, Y.O., Engel, H., van Besien, K., Giralt, S., Andersson, B., Kleine, H.D., Seong, D., Deisseroth, A.B., Andreeff, M., and Champlin, R. 1995. Allogeneic blood stem cell transplantation for refractory leukemia and lymphoma: potential advantage of blood over marrow allografts. *Blood* 85: 1659–1665.
 18. Nash, K., Chang, Q., Watts, A., Treter, S., Oravec, G., Ferrara, V., Buhler, L., Basker, M., Gojo, S., Sachs, D.H., White-Scharf, M., Down, J.D., and Cooper, D.K. 1999. Peripheral blood progenitor cell mobilization and leukapheresis in pigs. *Lab. Anim. Sci.* 49: 645–649.
 19. Negrin, R.S., Atkinson, K., Leemhuis, T., Hanania, E., Juttner, C., Tierney, K., Hu, W.W., Johnston, L.J., Shizurn, J.A., Stockerl-Goldstein, K.E., Blume, K.G., Weisman, I.L., Bower, S., Baynes, R., Dansey, R., Karanes, C., Peters, W., and Klein, J. 2000. Transplantation of highly purified CD34⁺Thy-1⁺ hematopoietic stem cells in patients with metastatic breast cancer. *Biol. Blood Marrow Transplant.* 6: 262–271.
 20. Norol, F., Merlet, P., Isnard, R., Sebillon, P., Bonnet, N., Cailliot, C., Carrion, C., Ribeiro, M., Charlotte, F., Pradeau, P., Mayol, J.F., Peinnequin, A., Drouet, M., Safsafi, K., Vernant, J.P., and Herodin, F. 2003. Influence of mobilized stem cells on myocardial infarct repair in a nonhuman primate model. *Blood* 102: 4361–4368.
 21. Primate Society of Japan. 1986. Guiding Principles for Animal Experiments Using Nonhuman Primates. *Primate Res.* 2: 111–113.
 22. Rosenfeld, C.S. 1993. A strategy for processing of peripheral blood stem cells utilizing the small volume collection chamber and cryopreservation without a rate controller using pentastarch. *J. Hematother.* 2: 525–528.
 23. Rowley, S.D., Prather, K., Bui, K.T., Appel, M., Felt, T., and Bensing, W.I. 1999. Collection of peripheral blood progenitor cells with an automated leukapheresis system. *Transfusion* 39: 1200–1206.
 24. Schmitz, N., Dreger, P., Suttrop, M., Rohwedder, E.B., Haferlach, T., Loffler, H., Hunter, A., and Russell, N.H. 1995. Primary transplantation of allogeneic peripheral blood progenitor cells mobilized by filgrastim (granulocyte colony-stimulating factor). *Blood* 85: 1666–1672.
 25. Schwella, N., Movassaghi, K., Scheduling, S., Ahrens, N., and Salama, A. 2003. Comparison of two leukapheresis programs for computerized collection of blood progenitor cells on a new cell separator. *Transfusion* 43: 58–64.
 26. Shibata, H., Hanazono, Y., Ageyama, N., Nagashima, T., Ueda, Y., Hasegawa, M., Ozawa, K., Yoshikawa, Y., and Terao, K. 2003. Collection and analysis of hematopoietic progenitor cells from cynomolgus macaques (*Macaca fascicularis*): assessment of cross-reacting monoclonal antibodies. *Am. J. Primatol.* 61: 3–12.
 27. Snyder, E.L., Baril, L., Cooper, D.L., Min, K., Mechanic, S., Stoddart, L., Burtess, B., Seagraves, P., Debelak, J., Gudino, M., and McCullough, J. 2000. *In vitro* collection and posttransfusion engraftment characteristics of MNCs obtained by using a new separator for autologous PBPC transplantation. *Transfusion* 40: 961–967.
 28. Sohn, S.K., Kim, J.G., Chae, Y.S., Kim, D.H., Lee, N.Y., Suh, J.S., and Lee, K.B. 2003. Large-volume leukapheresis using femoral venous access for harvesting peripheral blood stem cells with the Fenwal CS 3000 Plus from normal healthy donors: predictors of CD34⁺ cell yield and collection efficiency. *J. Clin. Apher.* 18: 10–15.
 29. Stamm, C., Westphal, B., Kleine, H.D., Petzsch, M., Kittner, C., Klinge, H., Schumichen, C., Nienaber, C.A., Freund, M., and Steinhoff, G. 2003. Autologous bone-marrow stem-cell transplantation for myocardial regeneration. *Lancet* 361: 45–46.
 30. Ueda, K., Hanazono, Y., Shibata, H., Ageyama, N., Ueda, Y., Ogata, S., Tabata, T., Nagashima, T., Takatoku, M., Kume, A., Ikehara, S., Taniwaki, M., Terao, K., Hasegawa, M., and Ozawa, K. 2004. High-level *in vivo* gene marking after gene-modified autologous hematopoietic stem cell transplantation without marrow conditioning in nonhuman primates. *Mol. Ther.* 10: 469–477.
 31. Witt, V., Fischmeister, G., Scharner, D., Printz, D., Pottschger, U., Fritsch, G., and Gardner, H. 2001. Collection efficiencies of MNC subpopulations during autologous CD34⁺ peripheral blood progenitor cell (PBPC) harvests in small children and adolescents. *J. Clin. Apher.* 16: 161–168.
 32. Woloskie, S., Armelagos, H., Meade, J.M., and Haas, D. 2001. Leukodepletion for acute lymphocytic leukemia in a three-week-old infant. *J. Clin. Apher.* 16: 31–32.
 33. Yoshino, N., Ami, Y., Terao, K., Tashiro, F., and Honda, M. 2000. Upgrading of flow cytometric analysis for absolute counts, cytokines and other antigenic molecules of cynomolgus monkeys (*Macaca fascicularis*) by using anti-human cross-reactive antibodies. *Exp. Anim.* 49: 97–110.
 34. Yoshioka, T., Ageyama, N., Shibata, H., Yasu, T., Misawa, Y., Takeuchi, K., Matsui, K., Yamamoto, K., Terao, K., Shimada, K., Ikeda, U., Ozawa, K., and Hanazono, Y. 2005. Repair of infarcted myocardium mediated by transplanted bone marrow-derived CD34⁺ stem cells in a nonhuman primate model. *Stem Cells* 23: 355–364.

Repair of Infarcted Myocardium Mediated by Transplanted Bone Marrow-Derived CD34⁺ Stem Cells in a Nonhuman Primate Model

TORU YOSHIOKA^{a,c}, NAOHIDE AGEYAMA,^f HIROAKI SHIBATA,^{a,f} TAKANORI YASU,^c YOSHIO MISAWA,^d KOICHI TAKEUCHI,^e KEIJI MATSUI,^c KEIJI YAMAMOTO,^c KEIJI TERAU,^f KAZUYUKI SHIMADA,^c UICHI IKEDA,^g KEIYA OZAWA,^{a,b} YUTAKA HANAZONO^a

^aCenter for Molecular Medicine; ^bDivision of Hematology, and ^cDivision of Cardiology, Department of Internal Medicine; ^dDivision of Cardiovascular Surgery, Department of Surgery; and ^eDepartment of Anatomy, Jichi Medical School, Minamikawachi, Tochigi; ^fTsukuba Primate Center, National Institute of Infectious Diseases, Tsukuba, Ibaraki; ^gDepartment of Organ Regeneration, Shinshu University Graduate School of Medicine, Matsumoto, Nagano, Japan

Key Words. Nonhuman primate • Acute myocardial infarction • Stem cell transplantation
Genetic marking • Lentivirus vector • Plasticity • Neovascularization

ABSTRACT

Rodent and human clinical studies have shown that transplantation of bone marrow stem cells to the ischemic myocardium results in improved cardiac function. In this study, cynomolgus monkey acute myocardial infarction was generated by ligating the left anterior descending artery, and autologous CD34⁺ cells were transplanted to the peri-ischemic zone. To track the *in vivo* fate of transplanted cells, CD34⁺ cells were genetically marked with green fluorescent protein (GFP) using a lentivirus vector before transplantation (marking efficiency, 41% on average). The group receiving cells (*n* = 4) demonstrated improved regional blood flow and cardiac function compared with the saline-treated group (*n* = 4) at 2 weeks after transplant. However, very few transplanted cell-derived,

GFP-positive cells were found incorporated into the vascular structure, and GFP-positive cardiomyocytes were not detected in the repaired tissue. On the other hand, cultured CD34⁺ cells were found to secrete vascular endothelial growth factor (VEGF), and the *in vivo* regional VEGF levels showed a significant increase after the transplantation. These results suggest that the improvement is not the result of generation of transplanted cell-derived endothelial cells or cardiomyocytes; and raise the possibility that angiogenic cytokines secreted from transplanted cells potentiate angiogenic activity of endogenous cells. STEM CELLS 2005;23:355–364

INTRODUCTION

Recent clinical studies have shown that the introduction of bone marrow cells can restore blood flow in ischemic myocardium and ameliorate cardiac function [1–6]. Despite

enthusiasm for these studies, it is unclear how transplanted bone marrow cells contribute to the clinical improvement. Because endothelial progenitor cells are identified in bone marrow cells [7], these cells might participate in the repair

Correspondence: Yutaka Hanazono, M.D., Ph.D., Division of Regenerative Medicine, Center for Molecular Medicine, Jichi Medical School, 3311-1 Yakushiji, Minamikawachi, Tochigi 329-0498, Japan. Telephone: 81-285-58-7450; Fax: 81-285-44-5205; e-mail: hanazono@jichi.ac.jp Received August 16, 2004; accepted for publication November 30, 2004. ©AlphaMed Press 1066-5099/2005/\$12.00/0 doi: 10.1634/stemcells.2004-0200

of vascular tissue. On the other hand, it has been reported that hematopoietic stem cells differentiate into endothelial cells and cardiomyocytes when transplanted into the ischemic myocardium in mice [8]. More recently, however, it has been reported that hematopoietic stem cells do not give rise to nonhematopoietic cells in the ischemic myocardium in murine models [9–11].

In vivo tracking and plastic properties of hematopoietic stem or progenitor cells have not been examined in primate cardiac ischemia. We have transplanted genetically marked autologous CD34⁺ cells to the ischemic myocardium in a nonhuman primate (*cynomolgus macaque*) model and tracked the in vivo fate of the cells. We have used CD34⁺ cells because the cells are widely used as a fraction of hematopoietic stem cells in clinical and nonhuman primate studies [12]. In addition, CD34⁺ cells contain vascular endothelial progenitor cells [7]. Thus, the present study can address the question of whether transplanted CD34⁺ cells really give rise to endothelial cells and cardiomyocytes in ischemic myocardium in primates.

MATERIALS AND METHODS

Animals

Eight *cynomolgus macaques* bred in the Tsukuba Primate Center (Ibaraki, Japan) were enrolled in the present study. This study strictly adhered to the rules for animal care and management of the Tsukuba Primate Center, as well as the guiding principles for animal experiments using nonhuman primates formulated by the Primate Society of Japan. The protocols of animal experiments were approved by the animal welfare and animal care committee of the National Institute of Infectious Diseases (Tokyo).

Preparation of CD34⁺ Cells

Cynomolgus bone marrow (50 ml) was aspirated from the iliac crest under an isoflurane-induced general anesthesia. From the bone marrow, a nucleated cell fraction was obtained after red blood cell lysis with addition of ACK buffer (Biosource, Camarillo, CA). CD34⁺ cells were isolated using magnetic beads conjugated with anti-human CD34 (clone 561; Dynal, Lake Success, NY), which cross-reacts with *cynomolgus* CD34 [13]. The purity of CD34⁺ cells at harvest ranged from 90% to 95%, as assessed with another anti-human CD34 (clone 563; PharMingen, San Diego) that cross-reacts with *cynomolgus* CD34 [13]. The purity remained at the same levels after the 1-day transduction culture, which is discussed next.

Lentiviral Transduction

A simian immunodeficiency virus (SIV)-based lentivirus vector carrying enhanced jellyfish green fluorescent protein (GFP) (Clontech, Palo Alto, CA) was used for transduction. The vector was prepared as previously reported [14, 15]. All recombinant DNA experiments were approved by the Ministry of Education, Culture, Sports, Science and Technology of Japan.

CD34⁺ cells (1×10^6) were seeded in six-well plates in 2 ml of StemSpan serum-free expansion medium (Stem Cell Technologies, Vancouver) supplemented with recombinant human thrombopoietin (100 ng/ml; Kirin, Tokyo), recombinant human stem cell factor (100 ng/ml; Biosource, Camarillo, CA), recombinant human Flt-3 ligand (100 ng/ml; Research Diagnostics, Flanders, NJ), and antibiotics (100 U/ml of penicillin and 0.1 µg/ml of streptomycin; Meiji, Tokyo). The cells were transduced twice each for 12 hours (total, 24 hours) with the SIV vector at 50 transducing units per target cell. After transduction, cells were cryopreserved with 10% dimethylsulfoxide (Wako, Osaka, Japan) and 1% Dextran 40 (Yoshitomi, Osaka, Japan) in a controlled-rate programmable freezer (Kryo 10; Planer Biomed, Middlesex, UK) until transplantation. The viability of cells after thawing was $53.0 \pm 6.5\%$, as assessed by trypan blue staining. An aliquot of transduced cells was assessed for GFP expression at 48 hours after transduction by flow cytometry using a FACScan (Becton Dickinson, Franklin Lakes, NJ) with excitation at 488 nm and fluorescence detection at 530 ± 30 nm.

In Vitro Endothelial Differentiation

CD34⁺ cells were seeded on fibronectin-coated plates (Becton Dickinson) in M199 medium (Invitrogen, Carlsbad, CA) with 20% fetal calf serum and bovine pituitary extracts (Invitrogen) as previously described [7]. After 7 days in culture, cells were examined for the uptake of DiI-acetylated low-density lipoprotein (LDL) and for the expression of CD31, von Willebrand factor (vWF), vascular endothelial (VE)-cadherin, and vascular endothelial growth factor receptor (VEGFR)-2. Briefly, adherent cells were incubated with 1 µg/ml of DiI-acetylated LDL (Molecular Probes, Eugene, OR) for 4 hours at 37°C. For immunofluorescence staining, after fixation in ice-cold 4% paraformaldehyde for 10 minutes and blocking in 1% bovine serum albumin (BSA) for 15 minutes, cells were incubated with a primary antibody: mouse anti-human CD31 (VM-59; Becton Dickinson), rabbit anti-human vWF (DakoCytomation, Glostrup, Denmark), mouse anti-human VE-cadherin (55-7H1; Becton Dickinson), or rabbit anti-mouse VEGFR2 (Santa Cruz Biotechnology, Santa Cruz, CA) for 1 hour at room

temperature. Cells were then incubated with a secondary antibody, Texas red-conjugated horse anti-mouse immunoglobulin G (IgG) (Vector, Burlingame, CA) or goat anti-rabbit IgG (Vector) for 30 minutes at room temperature.

Myocardial Infarction and Transplantation

All operations on cynomolgus monkeys were performed under an isoflurane-induced general anesthesia. Thoracotomy was conducted, the pericardium was opened, and the left anterior descending coronary artery was ligated with 5-0 prolene sutures. One to 2 hours after the ligation, GFP-transduced, autologous CD34⁺ cells in normal saline were injected with a microsyringe through a 27-gauge needle into 10 sites (5 μ l/site) in the peri-ischemic zone. In the control group, saline alone was injected in the same way. The pericardium and chest were closed. The animals then received butorphanol tartrate (0.5 mg/kg, intramuscularly) daily for 5 days to alleviate the pain associated with the operation and myocardial infarction.

Echocardiography

Echocardiographic imaging was obtained using a Sonos 5500 system (Philips Medical Systems, Andover, MA) before transplantation and at 2 weeks after transplant. The echocardiography was conducted by independent technicians irrelevant to our study group. In one animal (BM97080), it was additionally performed at 12 weeks. Short-axis two-dimensional images at the midpapillary level of the left ventricle were stored, and percent fractional shortening (%FS) was calculated to assess cardiac function.

Myocardial contrast echocardiography (MCE) was performed at day 0 (just before transplantation) and at 2 weeks after transplant to assess regional blood flow and blood flow defect size. In one animal (BM97080), chronic assessment was performed at 12 weeks after transplant. The electrocardiograph-triggered end-systolic intermittent imaging was conducted in short-axis views at incremental pulsing intervals (triggering intervals of 1, 2, 3, 4, and 8 beats) using an S12 probe. Once optimized, the settings of depth (4 cm), mechanical index (0.9), and focus (3 cm) were fixed. The contrast agent (perflutren; Yamanouchi, Tokyo) consisted of lipid-coated microbubbles of perfluorocarbon [16]. Perflutren diluted with saline (1:10) was administered intravenously at a constant rate (0.01 ml/kg per min). For the assessment of regional blood flow, MCE images were analyzed using ORIGIN 6.0J (Lightstone, Tokyo), and the blood flow was calculated as previously described [17]. Data are presented as a blood flow ratio (the peri-infarct versus nonischemic control region or the infarct versus nonischemic control region). For the assessment of blood flow defect, MCE images obtained at triggering interval of four beats were

analyzed using National Institutes of Health Image software (version 1.61). Data are presented as percent defect compared with the total blood flow.

Microspheres

Colored microspheres (15 μ m \pm 2% diameter; E-Z Trac, Los Angeles) were used to evaluate regional blood flow 2 weeks after transplant [18], with the exception of one animal (BM97080), in which evaluation was performed 12 weeks after transplant. A set of microspheres (2×10^6) was diluted in 2 ml of saline and injected into the left ventricle over 30 seconds. A reference blood sample was withdrawn at a constant rate of 5 ml/min through the femoral artery. After the collection of blood samples, monkeys were irrigated with saline for mercy killing and blood was completely washed out. The heart was excised from each monkey. Tissue samples from the infarct, peri-infarct, and nonischemic regions (one sample per region) were digested, microspheres were collected, and the blood flow was calculated according to the manufacturer's instructions. Data are presented as blood flow ratio (the peri-infarct versus nonischemic control region or the infarct versus nonischemic control region).

Immunohistochemistry

Tissue samples from the infarct, peri-infarct, and nonischemic regions at 2 weeks after transplant were embedded in optimal cutting temperature compound (Sakura, Zoeterwoude, Netherlands) and frozen in liquid nitrogen. Sections were prepared (6 μ m), fixed for 10 minutes at 4°C in 4% paraformaldehyde in phosphate-buffered saline (PBS), and blocked with 1% BSA in PBS. The sections were incubated at room temperature with a primary antibody, monoclonal mouse anti-human CD31 (1:200; Becton Dickinson), followed by a secondary antibody, biotin-conjugated horse anti-mouse IgG (1:500; Vector). The sections were then treated with avidin-alkaline phosphatase (ABC AP kit; Vector) for 30 minutes. The reaction was developed with a Vector Red substrate kit (SK-5100; Vector). In the case of double staining of CD31 and GFP, the above sections were further incubated with polyclonal rabbit anti-GFP (1:200; Clontech) followed by biotin-conjugated anti-rabbit IgG (1:500; Vector) and treated with avidin-peroxidase (ABC Elite kit; Vector). The reaction was developed with a Vector SG substrate kit (SK-4700; Vector). The sections were counterstained with hematoxylin, mounted in glycerol, and examined under a light microscope.

In Situ Polymerase Chain Reaction

In situ detection of transduced cell progeny was performed by amplifying proviral sequences as previously reported [19]. The following primer set for the GFP gene was used:

5'-CGT CCA GGA GCG CAC CAT CTT C-3' and 5'-GGT CTT TGC TCA GGG CGG ACT-3'. The polymerase chain reaction (PCR) mixture consisted of 420 μ M dATP, 420 μ M dCTP, 420 μ M dGTP, 378 μ M dTTP, 42 μ M digoxigenin-labeled dUTP (Roche, Mannheim, Germany), 0.8 μ M of each GFP primer, 4.5 mM MgCl₂, 1 \times PCR buffer (Mg²⁺ free), and 4 U of Takara Taq DNA polymerase (Takara, Kyote). Sections were prepared with a Takara slide frame (Takara) from the infarct, peri-infarct, and nonischemic regions at 2 weeks after transplant. PCR was performed using a PTC100 thermal cycler (MJ Research, Watertown, MA) with the following conditions: 94°C for 1 minute and 57°C for 1 minute with 10 cycles. The digoxigenin-incorporated DNA fragments were detected using horseradish peroxidase (HRP)-conjugated rabbit F(ab') anti-digoxigenin antibody (DakoCytomation). The sections were then stained for HRP using a Vector SG substrate kit (Vector). Finally, the sections were counterstained with a Kernechtrot solution (Muto, Tokyo) that stains nucleotides, mounted in glycerol, and examined under a light microscope.

ELISA

Vascular endothelial growth factor (VEGF) and basic fibroblast growth factor (bFGF) levels in tissue lysate or medium were assessed by ELISA (R&D Systems, Minneapolis) according to the manufacturer's instructions. Tissue lysate was obtained from the peri-infarct region (three samples from each monkey) at 2 weeks after transplant.

Briefly, tissue was homogenized and suspended in lysis buffer containing 10 mM Tris-HCl (pH 8.0), 1% Nonidet P-40, 150 mM NaCl, and protease inhibitor cocktail tablets (Complete Mini, Roche). The suspension was rocked at 4°C for 20 minutes and centrifuged at 16,000g and 4°C for 30 minutes. The supernatant was used for ELISA. The protein concentration of lysate was determined with DC Protein Assay (Bio-Rad, Hercules, CA).

RESULTS

Lentiviral Marking

The CD34⁺ fraction of autologous bone marrow cells was used for transplantation in our study (Table 1). Before transplantation, CD34⁺ cells were genetically marked with GFP using an SIV-based lentivirus vector. The ex vivo transduction results are summarized in Table 1. The transduced cells were frozen until transplantation. An aliquot of the transduced cells was examined in vitro for the endothelial differentiation ability. After the differentiation culture, a vessel-like structure was observed (Fig. 1A). The ability of cells to take up DiI-acetylated LDL and the expression of CD31, vWF, VE-cadherin, and VEGFR-2 suggested the endothelial lineage (Fig. 1B). We and others have already confirmed the ability of hematopoietic differentiation of the cells [20, 21]. Taken together, the SIV-mediated GFP gene transfer does not spoil the differentiation abilities of CD34⁺ cells. In addition, on average, 41% of cells fluoresced 48 hours after transduction, and 56% of

Table 1. Summary of ex vivo transduction and transplantation

	Sex	Age (y)	Body weight (kg)	Harvested bone marrow cell number	Isolated CD34 ⁺ cell number	Transplanted cell number	% GFP expression	
							Before ^a	After ^b
Saline group								
CTR01061 ^c	M	3	4.1			NA		
CTR99056	M	3	3.4					
CTR96116	F	5	3.2					
CTR99051	M	5	5.9					
CD34⁺ cell group								
BM01052	M	3	3.9	213 \times 10 ⁶	1.00 \times 10 ⁶	0.47 \times 10 ⁶	49	87
BM01051 ^d	M	3	4.1	396 \times 10 ⁶	5.14 \times 10 ⁶	2.20 \times 10 ⁶	51	54
BM97080 ^e	M	5	3.9	330 \times 10 ⁶	2.35 \times 10 ⁶	1.04 \times 10 ⁶	49	67
BM90047	M	13	5.8	343 \times 10 ⁶	3.10 \times 10 ⁶	1.07 \times 10 ⁶	16	14
Average		5	4.3	321 \times 10 ⁶	2.90 \times 10 ⁶	1.20 \times 10 ⁶	41	56

^aBefore endothelial differentiation of GFP-transduced CD34⁺ cells.

^bAfter the in vitro endothelial differentiation.

^cCTR01061 died of heart failure 5 days after myocardial infarction.

^dBM01051 developed a ventricular aneurysm after myocardial infarction.

^eBM97080 was killed 12 weeks after the treatment. All other animals were killed 2 weeks after the treatment.

Abbreviations: GFP, green fluorescent protein; NA, not applicable.

endothelial cells still fluoresced after in vitro differentiation (Table 1), showing that the GFP expression is stable during the in vitro differentiation to endothelial cells. Thus, GFP was expected to serve as a good genetic tag after transplantation.

Acute Myocardial Infarction and Autologous Transplantation

Cynomolgus acute myocardial infarction was generated by ligating the left anterior descending artery. One to two hours after the ligation, GFP-transduced, autologous CD34⁺ cells were injected in the peri-ischemic zone at 10 sites (total, $1.20 \pm 0.73 \times 10^6$ cells; $n = 4$). In the control group, saline was injected in the same way ($n = 4$). We conducted contrast echocardiography immediately after the coronary ligation and found no significant differences in the blood flow defect size (percent blood flow defect compared with the total) between the cell-treated and saline-treated groups ($13.0 \pm 2.1\%$ versus $12.3 \pm 3.5\%$, $p = .75$), suggesting that the initial risk of infarction did not differ between the two groups. In addition, we tried to assess the cardiac isozyme of serum creatine kinase (CK) to evaluate the infarct size; however, either the immuno-inhibition assay or chemical luminescence immunoassay did not work well for cynomolgus monkey samples. We were at least able to show that total CK values at 24 hours after the ligation did not significantly differ between the two groups ($p = .83$).

One of the control monkeys (CTR01061) died of heart failure 5 days after myocardial infarction, and the other control monkeys showed a decrease in %FS at 2 weeks after infarction (Fig. 2). Thus, all four control animals showed the deteriorated cardiac function. In the cell-treated group, one monkey (*, BM01051) underwent ventricular fibrillation immediately after the ligation and survived after cardiopulmonary resuscitation but eventually developed a ventricular aneurysm. Only this animal showed a decrease in %FS despite CD34⁺ cell treatment; the other animals receiving CD34⁺ cells showed an increase in %FS (Fig. 2). CD34⁺ cell treatment may not be able to rescue such a heavily impaired heart but otherwise had a significant effect on cardiac function. Even an old monkey (BM90047, Table 1) showed improved %FS.

The relative blood flow in the peri-infarct to nonischemic control region was also significantly ameliorated in the CD34⁺ cell-treated monkeys compared with the saline-treated ones, as assessed using contrast echocardiography (Fig. 3A) and colored microspheres (Fig. 3B). An excellent correlation was found between the two methods (Fig. 3C; correlation coefficient = 0.93). Two groups (CD34⁺ cell-treated and saline-treated) were well separated on the panel, showing an obvious positive effect of CD34⁺ cell injection on the blood flow in the peri-infarct zone after acute myocar-

dial infarction. In fact, the average myocardial blood flow in the peri-infarct region in the absolute value was 0.988 ml/g per minute and 0.383 ml/g per minute for the cell-treated and saline-treated groups, respectively. Of note, the blood flow in the peri-infarct zone was ameliorated even in the animal with a ventricular aneurysm. On the other hand, the relative blood flow in the infarct to nonischemic region did not show

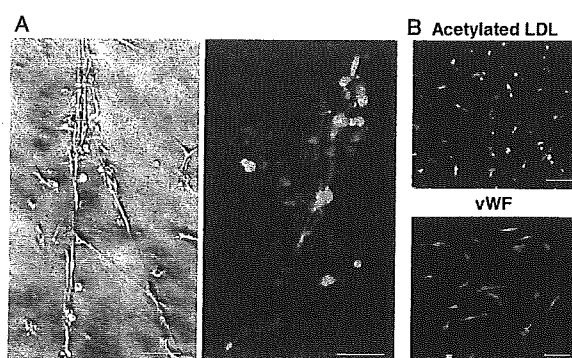


Figure 1. In vitro endothelial differentiation of cynomolgus CD34⁺ cells lentivirally transduced with GFP. The transduced CD34⁺ cells were differentiated to endothelial cells after 7 days in culture. (A): Representative vessel-like structure derived from CD34⁺ cells observed under a phase-contrast microscope (left) and a fluorescent microscope (right). (B): The transduced CD34⁺ cells differentiated into fluorescent cells (green) positive for the cellular intake of acetylated LDL and immunostaining for von Willebrand factor (vWF) (stained in red). Bar = 100 μ m. Abbreviations: GFP, green fluorescent protein; LDL, low-density lipoprotein.

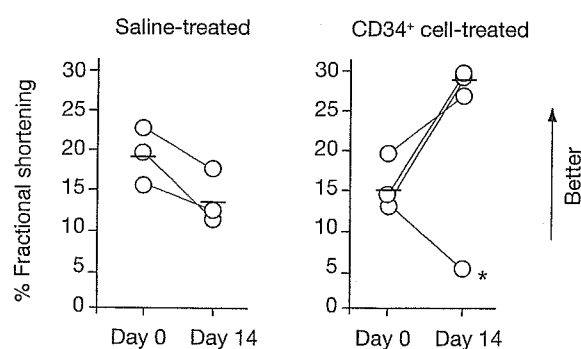


Figure 2. Improved cardiac function after CD34⁺ cell transplantation. Cardiac function was assessed by echocardiography in terms of percent fractional shortening (%FS) before and 2 weeks after treatment. One monkey in the saline-treated group (CTR01061) died of heart failure 5 days after myocardial infarction and is not included in the figure. One monkey in the CD34⁺ cell-treated group (*, BM01051) developed a left ventricular aneurysm after myocardial infarction. If this animal was excluded from the statistical analysis, the cardiac function was significantly improved in the CD34⁺ cell-treated compared with the saline-treated group in terms of the ratio of %FS at day 14 versus day 0 after transplant ($p = .017$).